PACS numbers: 42.55.Ks; 52.80.Hc
DOI: 10.1070/QE2000v030n08ABEH001800

Homogeneity and stability of volume electrical discharges in gas mixtures based on SF_6

Yu I Bychkov, S L Gorchakov, A G Yastremskii

Abstract. The electric parameters of the volume discharge and the transition of the discharge from the volume combustion to the channel stage are experimentally studied. It is shown that cathode spots of a hemispherical shape appear at the stage of the discharge formation. Over them, plasma plumes are developed which are combined to form a volume column of the discharge plasma. The discharge homogeneity increases with increasing density of the cathode spots. The distortion of the shape of cathode spots initiates the development of plasma channels. The development of the plasma channel is computer simulated. The results of calculations are discussed and compared with experimental data.

1. Introduction

The volume electric discharge in gas mixtures containing SF_6 is widely used to pump nonchain chemical HF lasers. In recent years, a high efficiency (above 3%) and a high specific output (6 – 8 J litre^{-1}) have been achieved for these lasers [1 – 3]. In Ref. [4], the possibility of creation of high-aperture lasers has been demonstrated.

The energy parameters of HF lasers can be further increased by improving pumping methods and optimising pumping conditions. A problem of pumping optimisation consists in obtaining required electric parameters of a discharge plasma by retaining its spatial homogeneity during a pump pulse. The discharge instability destroys its homogeneity and results finally in the transition of the discharge from the volume combustion to the channel stage (a contracted discharge). Physical processes resulting in the discharge instability remains poorly studied. The problem is also complicated by the fact that the discharge instability in different gases and gas mixtures is caused by different physical processes.

The gas mixture in HF lasers consists of SF_6 and additions of hydrogen donors (H_2, C_2H_6 or other hydrocarbons). For this reason, it is of interest to study the discharge properties both in the laser mixture and pure SF_6. The properties of a homogeneous discharge have been described in detail in Refs [5, 6]. In this paper, we studied experimentally the electric parameters of the contracted discharge plasma, the contraction process itself, and the development of a single plasma plume. Also, the formatrion of a plasma channel was simulated.

Yu I Bychkov, S L Gorchakov, A G Yastremskii Institute of High-Current Electronics, Siberian Division, Russian Academy of Sciences, Akademicheskii prosp. 4, 634055 Tomsk, Russia

Received 26 January 2000
Kvantovaya Elektronika **30** (8) 733 – 737 (2000)
Translated by M N Sapozhnikov

2. Experimental results and discussion

We used in our experiments a scheme of the discharge photoinitiation suggested in Refs [5, 6]. The disharge diagnostics included the detection of the discharge current and voltage across the plasma channel, as well as photographing of the integrated discharge emission and the cathode surface.

2.1. Development of the high-conduction cathode spot channels

We studied the discharge transition from the volume to channel stage in the $Ne - SF_6 - C_6H_{14}$ mixture. The discharge area was 10 cm^2 and the interelectrode distance was 3.8 cm.

In the $Ne : SF_6 : C_6H_{14}$ = 45 : 3 : 11 Torr mixture, the incomplete high-conduction channels directed towards an anode (plasma channels) began to develop at a current density of $\sim$ 600 A cm^{-2} (Fig. 1a). In the interelectrode space, the plasma remained highly homogeneous. An increase in the current density up to 700 A cm^{-2} (Fig. 1b) resulted in a further development of incomplete channels directed towards an anode, the appearance of anode spots and incomplete channels directed towards a cathode. For the current density above 750 A cm^{-2} (Fig. 1c), the channels directed

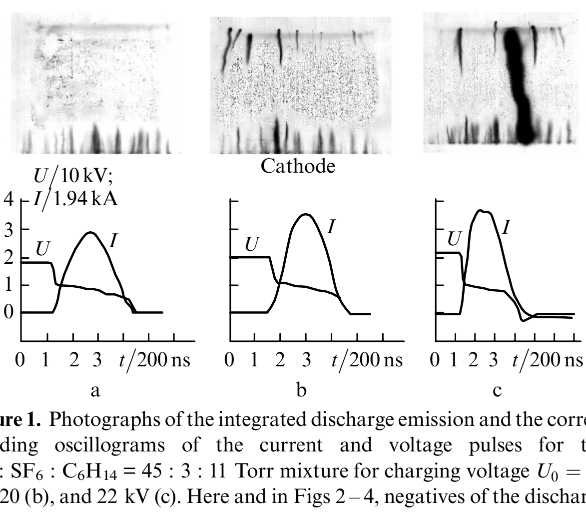

Figure 1. Photographs of the integrated discharge emission and the corresponding oscillograms of the current and voltage pulses for the $Ne : SF_6 : C_6H_{14}$ = 45 : 3 : 11 Torr mixture for charging voltage U_0 = 18 (a), 20 (b), and 22 kV (c). Here and in Figs 2 – 4, negatives of the discharge emission are presented.

to the anode and cathode merged. During the overlap of the discharge gap by the plasma channel (Fig. 1c) the voltage at the pulse end abruptly falls due to an increase in the channel conduction.

Fig. 2 shows photographs of the discharge integrated emission and oscillograms of current pulses I and plasma voltage U for the Ne : SF_6 : C_6H_{14} = 45 : 11 : 11 Torr mixture at an increased partial pressure of SF_6. For a discharge capacitor with the capacitance $C = 23$ nF and the charging voltage $U_0 = 30$ kV (Fig. 2a), the current density was 700 A cm^{-2}, the voltage across a plasma channel at the current maximum was 15 kV, and the pulse duration (over its base) was 250 ns. A high density of cathode spots was observed, from which incomplete channels started to develop, and the discharge column was highly homogeneous.

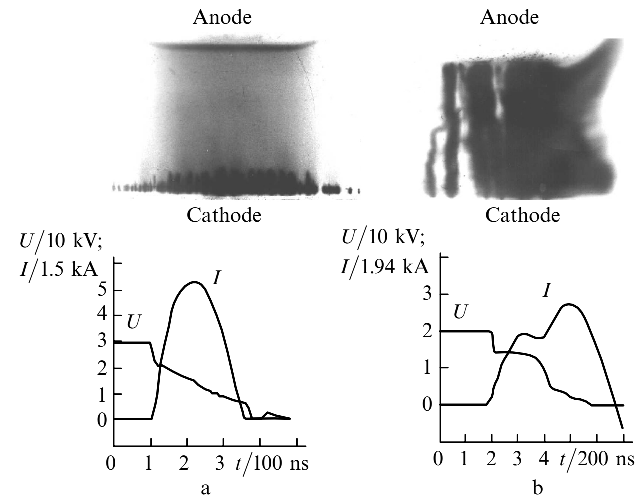

Figure 2. Photographs of the integrated discharge emission and the corresponding oscillograms of the current and voltage pulses for the Ne : SF_6 : C_6H_{14} = 45 : 11 : 11 Torr mixture at $U_0 = 30$ (a) and 20 kV (b); $C = 23$ (a) and 92 nF (b).

In the matched pumping regime, the specific energy input of about 0.6 J cm^{-3} was achieved, which is maximum for a given mixture in the homogeneous combustion stage. The pulse duration could be increased upon retaining the homogeneity only by decreasing the current density.

As the capacitor capacity was increased to 92 nF, a great number of plasma channels appeared in the discharge plasma (Fig. 2b), which had a comparatively large diameter ($\sim$ 1 cm). The time separation of the volume and channel discharge stages is distinctly observed on the oscillograms of current pulses and voltage across the plasma channel. The volume stage continues for 400 ns. During this stage, the voltage across a plasma remains equal to $U = 15$ kV. Then, it abruptly falls to 5 kV and after that smoothly decreases. The discharge passes to the multichannel stage, which is not typical for electric discharges in other gas mixtures. The time dependence of the discharge current exhibits two characteristic maxima corresponding to the volume and channel stages of the discharge.

The above results give the following sequence of the events taking place during the discharge development: The appearance of cathode spots at the initial stage of the discharge, the development of incomplete channels directed to the anode, the formation of incomplete channels directed to the cathode, and merging of the counter channels accompanied by an increase in their conduction.

2.2. Study of separate plasma plumes

We studied separate plasma spots and plasma plumes in the SF_6 gas at a pressure of 45 Torr. To produce a single plasma spot, we covered the cathode surface with a dielectric with a hole in it 0.04 cm in diameter. The interelectrode distance was 2.6 cm.

The discharge developing under such conditions is shown in Fig. 3. One can see that the produced cathode spot has a hemispherical shape (Fig. 3a), which is retained at a larger current of 1 kA (Fig. 3b). The diameter of the hemisphere is an order of magnitude larger than the hole diameter in a dielectric. A distinct boundary between the hemisphere and the plasma plume is observed. As the current increased by a factor of four, the hemisphere diameter increased by a factor of one and a half. An increase in the capacity of the discharge capacitor by a factor of two (Fig. 3c) at the 1.5 kA current resulted in the distortion of the hemispherical shape and the development of the incomplete plasma channel directed to the anode.

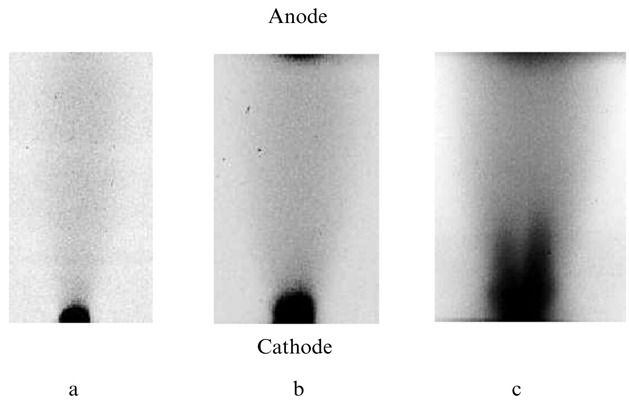

Figure 3. Photographs of the integrated emission of a single plasma plume for the discharge current $I = 300$ (a), 1000 (b) and 1500 A (c) and energy inputs $E_{in} = 0.2$ (a), 0.4 (b), and 1 J (c).

Fig. 4 shows the discharge consisting of three plasma plumes formed from three cathode spots spaced at 1.5 cm intervals. Capacities of the capacitors were 2.26 nF (Fig. 4a) and 4.52 nF (Figs 4b, c); the other conditions were as in Fig. 3.

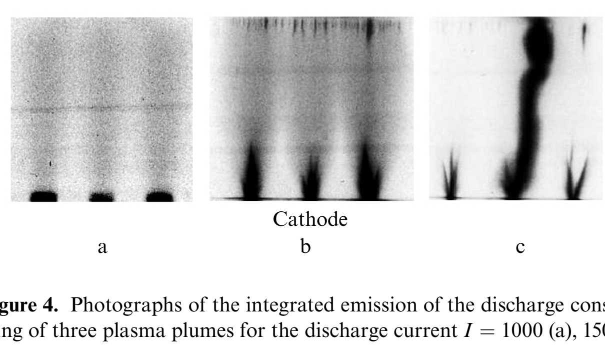

Figure 4. Photographs of the integrated emission of the discharge consisting of three plasma plumes for the discharge current $I = 1000$ (a), 1500 (b), and 2000 A (c) and energy inputs $E_{in} = 0.4$ (a) and 2 J (b, c).

In Fig. 4a, each spot experiences a 300 A current flow, and a distinct boundary between the cathode spot and the discharge plasma is observed. As the current increases (Fig. 4b), the incomplete channels directed to the anode are developed, and many narrow incomplete channels directed to the cathode appear on the anode. As the current further increases through one channel up to ~ 700 A (Fig. 4c), one or two plasma channels appear, which close the electrodes.

Comparison of the results presented in Figs 3 and 4 shows that the adjacent cathode spots affect each other. The channels begin to develop at a substantially lower current flowing through one spot. Indeed, in the case of a single cathode spot, the channel development occurs at $I = 1.5$ kA (Fig. 3c), whereas in the case of three cathode spots, the channels develop already at a current through a channel equal to 500 A (Fig. 4b). The critical current density decreases with increasing number of spots. Thus, we obtained a highly homogeneous discharge in pure SF_6 at the spot density equal to 20 cm^{-2}. The channels began to develop at a current density of about ~ 400 A cm^{-2}, and, therefore, a high spot density leads to the channel formation at a comparatively low current (~ 20 A) flowing through a spot.

Therefore, to improve the homogeneity of the plasma discharge, one should increase the density of cathode spots. However, one should take into account that in this case, the current flowing through one spot, at which the channel 'intergrowth' begins, simultaneously automatically decreases. Note that a plasma channel is formed from a cathode spot at some critical values of the electric field strength and the current density at the interface between the spot and the plasma plume. The experimental results suggest that the current density and the electric field strength at the top of the cathode spot increase with increasing discharge current much more rapidly at the high spot density.

3. Simulation of the plasma channel 'intergrowth'

3.1. Description of the model

To simulate the discharge contraction process numerically, we developed a self-consistent discharge model, which included Boltzmann equations describing the electron kinetics, a system of balance equations describing the time dependence of the concentration of active particles in a plasma, the equation for the temperature of an active medium, and a system of equations for an external electrical circuit.

The simulation was performed for the mixture $Ne : SF_6 : C_6H_{14} = 45 : 11 : 11$ Torr. The processes involving a hexane molecule were described using the data base for cross section for elementary processes for ethane. The ionisation cross section for ethane was modified as in Ref. [7]. The kinetic model contains the equations describing the time dependence of concentrations of electrons, neon atoms in the ground and excited states, SF_6 molecules in the excited electronic states, SF_6 molecules in the excited vibrational states ($v = 0, 1$), hydrocarbon molecules, and also atomic and molecular ions (Ne^+, $C_6H_{14}^+$, F^-, F_2^-, SF_4^-, SF_5^-, SF_6^-, SF_6^+, and SF_5^+). In addition, the model takes into account the time dependences of concentrations of neutral atoms and molecules (SF_5, SF_4, F, F_2, HF, C_2H_4, H_2, H, etc.) Basic kinetic processes, the values of rate constants and cross sections were taken from [1, 8].

Unlike other models, our model takes into account step ionisation of SF_6 and SF_5 molecules. Because the data on cross sections for step ionisation of SF_6 and SF_5 molecules are not available in the literature, we used for estimates the modified cross section for step ionisation of Xe, which has a threshold of 6 eV. This cross section achieves the maximum value of about $\sim 3 \times 10^{-15}$ cm^2 at the energy ~ 10 eV.

One of the important features of the discharge in SF_6 is a rapid increase in the concentration of electrons and ions at the initial moment. For this reason, to provide the required accuracy of calculations, we used the nonstationary Boltzmann equation in our model, which was solved by the method of weighted residuals [9]. The system of balance equations and equations of the electric circuit was solved by the Gear method.

The discharge contraction process was simulated by decreasing the discharge area from 10 to 1 cm^2 for 20 ns at the moment of maximum current. We assumed that all the channels observed experimentally are replaced by a single channel with a specified discharge area. The channel was assumed to be homogeneous over the interelectrode distance. An increase in the channel conduction was calculated self-consistently.

3.2. Simulation results

The results of simulation of time dependences $U(t)$ and $I(t)$ during the channel formation are presented in Fig. 5. Our calculations qualitatively agree with the experimental data. They correctly predict the presence of two maxima of the discharge current and a rapid fall of the voltage during the discharge formation and upon the transition to the channel discharge stage.

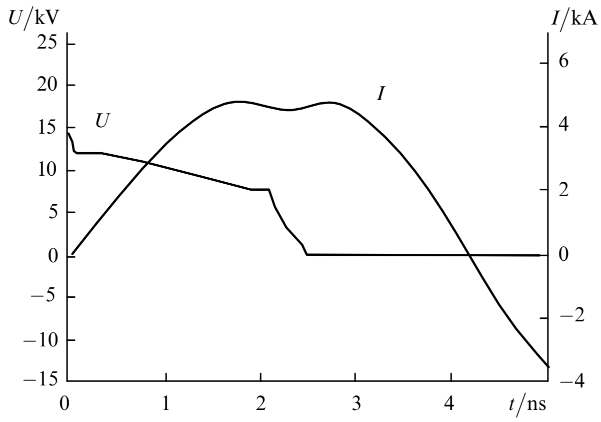

Figure 5. Calculated time dependences of the discharge current I and voltage U for the $Ne : SF_6 : C_6H_{14} = 45 : 11 : 11$ Torr mixture for $U_0 = 20$ kV, $C = 92$ nF, $S = 10$ cm^2, and $d = 3.7$ cm.

Fig. 6a shows the calculated time dependences of concentrations of electrons (n_e) and positive and negative ions SF_6^+ and SF_5^-. At the initial discharge stage, the concentrations of charged particles rapidly increase. The concentrations increase exponentially with the characteristic rise time shorter than 10^{-9} s, and increase by five orders of magnitude for 15 ns. In the time interval between 15 and 50 ns, the rate of increase in the electron concentration slows down. The reason for its slowing down is explained in Fig. 6b, which shows that in this time interval, the concentration of the $SF_6(1)$ molecules rapidly increases, resulting in the increase in the attachment frequency.

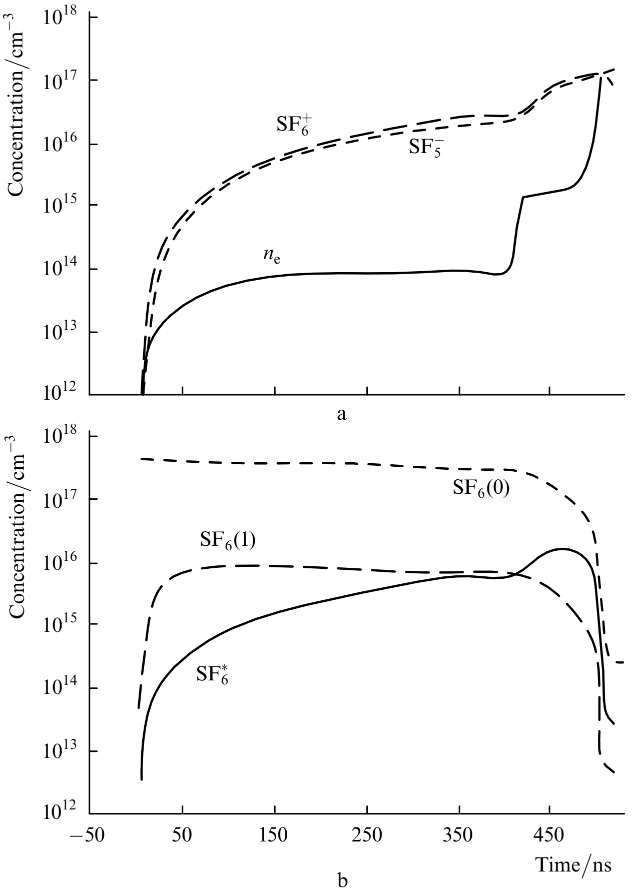

Figure 6. Calculated time dependences of concentrations of electrons and ions SF_6^- and SF_5^- (a) and concentrations of SF_6 molecules in the ground and excited states (b) for the Ne : SF_6 : C_6H_{14} = 45 : 11 : 11 Torr mixture for $U_0 = 20$ kV, $C = 92$ nF, $S = 10$ cm^2, and $d = 3.7$ cm.

In the discharge, a state is established for 400 ns during which the voltage across the plasma channel gradually decreases (Fig. 5). Charged particles produced due to the step ionisation, which weakly depends on U, cause a rapid increase in the concentration of SF_6^* molecules. Concentrations of $SF_6(0, 1)$ molecules decrease because of their conversion to SF_5^- molecules caused by dissipative electron attachment. The ion concentration at the current maximum proves to be two orders of magnitude greater than that of electrons (Fig. 6a). The plasma becomes ion in its charge composition. However, the electric current remains mainly electronic because the electron drift velocity is three orders of magnitude greater than that of ions.

To the moment of the discharge contraction ($t = 400$ ns), the current density and the electron concentration in a plasma amount to 500 A cm^{-2} and 10^{14} cm^{-3}, respectively. The discharge contraction caused an increase in the plasma resistance, resulting in the increase in the voltage across the plasma channel at a constant current (a rapid variation of the current was prevented by an inductance). A small increase in the voltage U was sufficient to increase the electron concentration and the current density by an order of magnitude. Our calculations showed that the increase in the current in the plasma channel is caused by the step ionisation of SF_6 molecules. Because the $SF_6(0,1)$ molecules have not been substantially burnt out (Fig. 6b), the rate of the electron concentration increase after its jump again slows down at $n_e \sim 10^{15}$ cm^{-3} ($t = 420$ ns). The initial voltage across the plasma channel in the combustion regime remained large $U(t = 420 \text{ ns}) = 8$ kV. This caused a repeated increase in the electron concentration and a decrease in the concentration of $SF_6(0,1)$ molecules by three orders of magnitude. In the time interval between 420 and 500 ns, the electron concentration increases, the channel conduction increases and the voltage across it decreases. At the concentration $n_e \geqslant 10^{17}$ cm^{-3}, processes of the establishment of thermodynamic equilibrium proceed in the plasma, which are not considered in our model.

The results of our calculations allow us to indicate a number of factors of interest for analysis of processes of the channel formation in a real discharge:

(1) The current density in a channel at the initial stage of its formation increases upon decreasing the discharge area, at a constant total discharge current, and upon a weak increase in the voltage across the plasma channel.

(2) For the current density equal to 500 A cm^{-2} ($n_e = 10^{14}$ cm^{-3}), a small increase in electric field strength in the region of the channel formation increases the ionisation frequency and results in the increase in the electron concentration.

(3) The high-conduction channel is formed at the final stage at a critical electron concentration ($n_e = 10^{15}$ cm^{-3}), at which the frequency of dissipative attachment decreases and the avalanche increase in the step ionisation frequency is achieved.

The above model of the discharge formation does not reflect the real dynamics of the development of the plasma channel from a cathode spot. The model gives a qualitative picture of the physical processes involved. Our experiments showed that the channels develop from cathode spots at the current density in the volume discharge of 400 – 500 A cm^{-2}. At the boundary between the cathode spot, which has initially a hemispherical shape, and the plasma plume, the electric field strength and the current density exceed their mean values in the discharge plasma. When the critical current density is achieved, the hemispherical shape of the cathode spot is distorted and a channel starts to develop. The electric field strength and the current density at the channel top further increase. In the plasma plume over the developing channel, the processes described by our model should proceed. As a result, the channel will develop and move from a cathode to an anode.

4. Conclusions

The main results of our paper are as follows:

(1) Hemispherical cathode spots of a typical size 0.1 cm appear at the initial stage of the discharge formation. At the homogeneous discharge stage at the current density up to 400 – 500 A cm^{-2}, the cathode spots retain their hemispherical shape.

(2) The distortion of the hemispherical shape of the cathode spot is the beginning of the development of the plasma channel. In the case of separate cathode spots, the channel starts to form at the total current flowing through one spot above 1000 A. The distortion of the hemispherical shape of cathode spots in the volume discharge with a high density of cathode spots (~ 20 cm^{-2}) occurs at a substantially lower current flowing through one spot (~ 20 A). An increase in the cathode spot density improves the discharge homogeneity but reduces the current through a spot at which the hemispherical spot shape is distorted and the channel formation begins.

(3) The development of an incomplete channel directed towards the anode initiates the appearance of incomplete channels on the anode. The counter developing channels merge to produce a plasma channel connecting the electrodes.

(4) Our calculations showed that upon the development of the channel directed towards the anode, a small increase in the electric field strength at its top results in an abrupt increase in the current density caused by step ionisation. The region of the raised electric field strength moves and the channel advances to the anode. At the second stage, the counter developing channels merge to produce a plasma channel connecting the electrodes. The basic processes proceeding in the channel are the step ionisation, attachment, and decomposition of the $SF_6(0,1)$ molecules. These processes provide an increase in the channel conduction at the decreasing voltage.

References

1. Richeboeuf L, Pasquires S, Legentil M, Puech V *J. Phys. D* **31** 373 (1998)
2. Tsikrikas G N, Serafetinides A A, Papayannis A D *Appl. Phys. B* **62** 357 (1996)
3. Anderson N, Bearpark T, Scott S J *Appl. Phys. B* **63** 565 (1996)
4. Apollonov V V, Kazantsev S Yu, Oreshkin V F, Firsov K N *Kvantovaya Elektron. (Moscow)* **25** 123 (1998) [*Quantum Electron.* **28** 116 (1998)]
5. Bychkov Yu, Gorchakov S, Lacour B *Proc. SPIE-Int. Soc. Opt. Eng.* **3403** 82 (1998)
6. Bychkov Yu I, Gorchakov S L, Yastremskii A G *Izv. Vyssch. Uchebn. Zaved., Fiz.* No. 8 43 (1999)
7. Beran J A, Kevan L *J. Phys. Chem.* **73** 3866 (1969)
8. Yastremskii A G, Yampol'skaya S A *Izv. Vyssch. Uchebn. Zaved., Fiz.* No. 8 63 (1999)
9. Fletcher C A J *Computational Galerkin Methods* (New York: Springer-Verlag, 1984) [Russ. transl., Moscow: Mir, 1988]